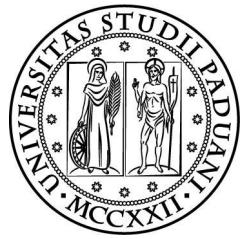

Università degli Studi di Padova

Dipartimento di Ingegneria dell'Informazione

Tesi di Laurea Magistrale

Approximate Solution to the Reactive Power Flow and its Application to Voltage Stability in Microgrids

Basilio Gentile
Ingegneria dell'Automazione
Anno Accademico 2012-2013

Relatore:
Prof. Sandro Zampieri

Correlatori:
Prof. Kai Heussen (Danmarks Tekniske Universitet)
Prof. Francesco Bullo (University of California Santa Barbara)

October 9, 2013

Summary

This work focuses on reactive power flow and voltage stability in electrical grids. We provide novel analytical understanding of the solutions to the classic quadratic equations describing the decoupled reactive power flow. As of today, solutions to these equations can be found only via numerical methods. Yet an analytical understanding would help rigorous design of future electrical grids.

The work presents two main contributions. First, for sufficiently-high source voltages, we guarantee the existence of a high-voltage solution for the reactive power flow equations and provide its approximate analytical expression. This result takes inspiration and extends the work proposed by [1]. We derive a bound on the approximation error and study its asymptotic behavior for large source voltages; we validate the accuracy of our approximation through the numerical study of the IEEE 37 test case. Second, we consider a recently-proposed droop control strategy for voltage stabilization in a microgrid equipped with inverters. We apply our previous result to the closed loop system: for sufficiently-high reference voltages, we prove the existence and provide an approximate expression of a high-voltage fixed point. Finally, we prove the local exponential stability of the fixed point and validate our results through a numerical analysis on the IEEE 37 grid.

The thesis work was carried out at the University of California Santa Barbara, in the research group supervised by Professor Francesco Bullo.

Acknowledgements

I gratefully acknowledge Professor Sandro Zampieri, Professor Kai Heussen and Professor Francesco Bullo for their assistance and guidance in the thesis project.
This thesis is based on the contents of a paper that I, John Simpson Porco, Florian Dörfler, Sandro Zampieri and Francesco Bullo submitted to the American Control Conference 2014. I am very grateful to the co-authors of the paper for the joint work of the last months, which helped me significantly in writing this Master's thesis.
I express my gratitude to all the mathematics teachers of my life, because they succeeded in transmitting to me a big passion; in particular I mention my first elementary school teacher Lucia, who is not here any more.
Special thanks to my mum and my dad, because through their example and direct help they always marked the importance of pursuing a good education with application and curiosity.
I am grateful to all the friends that I found in my studies; through long and deep discussions they helped my growth as a student and increased my excitement for the subjects. In particular I thank Giulia, who shared with me a big portion of the study effort and of the adventures in the three semesters at DTU.
Finally I am thankful to my brother Filippo and all my friends, in Italy and in the world, who make my life so wonderful.

Contents

Chapter 1

Introduction

The power flow equations model the relationships among bus power injections, power demands, and bus voltage magnitudes and angles in a power network. They are the heart of most system-planning and operational studies and also the starting point for transient and dynamic stability studies. They constitute a set of coupled equations with trigonometric and polynomial non-linearities, and the solution space admits a rich and complex phenomenology [2, 3]. Conditions for the existence and exact expression of the solutions have been derived for the case of a radial grid [4], while for a general network only conservative conditions have been proposed [5–7]. As of today, the power flow equations are solved numerically [8] and the power industry puts a considerable effort for the simulation of thousands of power flow equations for large grids. This motivates the importance of a deeper analytic insight into the problem.

A classic approach [5, 6] to the analysis of the power flow equations is to study the active and the reactive power equations separately under mild decoupling assumptions which are usually satisfied under regular system operation [9]. After the decoupling, the phase angles become the only variables appearing in the active power equations, while the voltage magnitudes become the only variables in the reactive ones. We focus our attention on the resulting reactive power flow equations: these are a system

of quadratic equations in the voltage magnitudes at the buses. Despite the simpler problem formulation, no sharp analytic answers pertaining to the existence of solutions are known to date [5–7].

The first contribution of this work is an approximate solution to the reactive power flow equations. This solution is the reactive counterpart of the DC approximation for the active power flow [10]. The DC approximation expresses the solution to the non-linear active flow equations as a linear combination of the active powers at the buses. The linear coefficients only depend on the network parameters. The approximate solution that we propose for the reactive power flow is the sum of two main terms: the first one is similar to the DC approximation, as it is a linear combination of the reactive powers at the buses; the linear coefficients only depend on the network parameters. The second term consists of a constant high-voltage value for each bus, and it is related to the general and well accepted idea that strongly-clustered high-voltage solutions of the reactive flow equations are the desired stable solutions [11].

In the second part of the work we focus on the stability of a droop control strategy in an islanded microgrid. Microgrids are low-voltage electrical distribution networks, heterogeneously composed of distributed generation, load, and managed autonomously from the larger primary network. Power sources in microgrids generate either variable frequency AC power or DC power, and are interfaced with a synchronous AC microgrid via power electronic DC/AC *inverters*. In islanded operation, it is through these inverters that actions must be taken to ensure synchronization, voltage stability, power balance and load sharing in the network [12]. We consider the problem of voltage stabilization; that is, keeping the average voltage level in the network high, and keeping the total voltage profile roughly uniform. This is a crucial aspect of microgrid control, as the relatively low voltage levels and uncompensated loads in microgrids put the network at risk for voltage instability and collapse [3]. In the last

two decades the $E-Q$ voltage-droop controller has become the tool commonly used for these tasks [13]. Despite the wide-spread adoption of the $E-Q$ voltage-droop controller, few analytic results are available about its closed-loop performance. Specifically, to the best of our knowledge, no results are available on the existence and locations of the equilibria of the closed-loop network. This work considers the *quadratic droop controller* proposed by [14]. This modified version of the standard $E-Q$ droop controller reproduces the inherently quadratic and asymmetric nature of the reactive power flow equations and facilitates an analytic treatment. The work carried out it [14] characterizes the existence, stability and location of the equilibrium point for a purely-inductive (lossless) network with parallel topology. In this work, we consider networks with arbitrary topology and with arbitrary heterogeneous (resistive and inductive) impedences; by applying the approximation method proposed for the reactive power flow equations, this work establishes the existence and the stability of a high-voltage fixed point and provides an approximate expression for its location.

This thesis is organized as follows. In Chapter 2 we review some background necessary for the rest of the work and introduce the reactive power flow equations. Chapter 3 defines the approximate solution to the reactive power flow equations. Chapter 4 applies the approximation method to a droop-controlled microgrid. Chapter 5 contains our concluding remarks.

Chapter 2

Background

In this Chapter we illustrate some preliminary concepts that are needed to formulate the problem in a rigorous way and to understand the techniques used to derive our results. The first part of this Chapter introduces basic notions of graph theory and multivariate analysis. The second part of this Chapter describes some general aspects of the power grid relevant to our work and presents the model of the grid used throughout the rest of the text.

2.1 Mathematical preliminaries

The thesis has a mathematical nature. To easily understand the rest of the work, it is necessary to introduce some notation that will be used throughout the text. Moreover, the study conducted is based on a *network theoretical* approach of the power grid, therefore some basic notions and results of graph theory are introduced. We conclude this Section by presenting a classical tool in non-linear analysis, the *implicit function theorem*, because it will be the core of the proofs of the two main results of the thesis.

Notation

Given a finite set $\mathcal{V}$, let $|\mathcal{V}|$ denote its cardinality. Let $\mathbb{1}$ denote the vector of all ones, $\mathbf{0}$ a matrix of all zeros; their dimension is not specified as it is understandable from the context. We do not specify the dimension of the identity matrix I either. Let $[x_i]_{i\in\mathcal{V}}$ be an alternative notation for the vector x, with indices in the set $\mathcal{V} = \{1, \dots, n\}$. Let $\text{diag}(x)$ denote the diagonal matrix whose diagonal is formed by the entries of the vector x and $\text{diag}^{-1}(x)$ its inverse, when defined. Given the vectors x and y, we write $x > y$ (resp. $x \geq y$) if $x_i > y_i$ (resp. $x_i \geq y_i$), for all i. For $a \in \mathbb{C}$, a^* denotes the complex-conjugate of a. Given the functions $f, g : \mathbb{R} \to \mathbb{R}$, we say that $f \in o(g)$ if $\lim_{x\to\infty} f(x)/g(x) = 0$.

Graph theory concepts

We define a *graph* $\mathcal{G}$ to be a pair $(\mathcal{V}, \mathcal{E})$, where $\mathcal{V}$ is a non-empty finite set of elements called *vertices*, and $\mathcal{E} \subset \mathcal{V} \times \mathcal{V}$ is a finite set of ordered pairs of distinct elements of $\mathcal{V}$ called *edges*. Let us define two functions $\sigma, \tau : \mathcal{E} \to \mathcal{V}$ such that $e = (\sigma(e), \tau(e))$ for each $e \in \mathcal{E}$, i.e., such that edge e connects node $\sigma(e)$ to node $\tau(e)$. We call node $\sigma(e)$ the *source* and node $\tau(e)$ the *terminal* of edge e. Since the edges are ordered pairs, we say that $\mathcal{G}$ is a *directed* graph. We define a *path* as an ordered sequence of edges $(e_{i_1}, e_{i_2}, \dots, e_{i_k})$ such that, for each pair of consecutive edges e_{i_j} and $e_{i_{j+1}}$ in the sequence, we have that $\tau(e_{i_j}) = \sigma(e_{i_{j+1}})$. We say that the graph is *strongly connected* if there exists a path connecting any two of its nodes. Throughout the text we will only consider strongly connected graphs. In Figure 2.1 we report a four node directed graph.

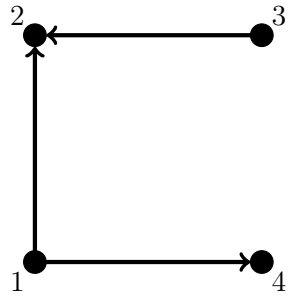

Figure 2.1: A four node directed graph.

The *incidence* matrix $B \in \{0, \pm 1\}^{|\mathcal{E}| \times |\mathcal{V}|}$ specifies which pair of nodes an edge is connecting and is defined as

$$[B]_{ev} = \begin{cases} -1 & \text{if } v = \sigma(e) \\ 1 & \text{if } v = \tau(e) \\ 0 & \text{otherwise .} \end{cases}$$

The incidence matrix of the graph in Figure 2.1 is

$$B = \begin{bmatrix} -1 & 0 & 1 & 0 \\ -1 & 1 & 0 & 0 \\ 0 & 1 & -1 & 0 \end{bmatrix}$$

We introduce a real *weight function* W on the edges $\mathcal{E}$ of the graph

$$\begin{aligned} W : \ \mathcal{E} &\to \mathbb{R} \\ (i, j) &\mapsto w_{ij} \ . \end{aligned}$$

The weight function W associates a real number to each edge. The graph $\mathcal{G}$ equipped with the function W is called undirected *weighted* graph and is referred to as $\mathcal{G}(\mathcal{V}, \mathcal{E}, W)$. We define its *Laplacian* matrix $L \in \mathbb{C}^{|\mathcal{V}| \times |\mathcal{V}|}$ as

$$[L]_{ij} := \begin{cases} -w_{ij} & \text{for } i \neq j \\ \sum_{k \neq i} w_{ik} & \text{for } i = j \ , \end{cases} \tag{2.1}$$

where formally we set $w_{ij} = 0$ if $(i, j) \notin \mathcal{E}$. So far we considered the case of a directed graph, where a direction is assigned to each edge. We introduce now the notion of *undirected* graph, where edges do not possess a direction. An undirected graph is defined as a directed one, but with the further requirement that if $(i, j) \in \mathcal{E}$ then it is also $(i, j) \in \mathcal{E}$. That is to say, an undirected edge from i to j can be thought as two directed edges, one from i to j and the other from j to i. If a weight function is defined on $\mathcal{G}$, we require that $w_{ij} = w_{ji}$. It follows that the Laplacian matrix of an undirected graph is *symmetric*. Figure 2.2 shows an example of undirected, weighted graph.

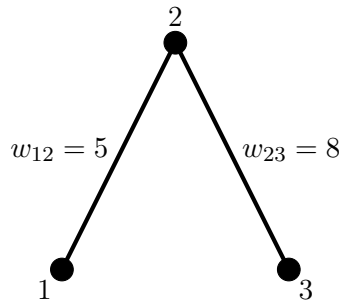

Figure 2.2: A three node undirected weighted graph.

Its Laplacian matrix is

$$L = \begin{bmatrix} 5 & -5 & 0 \\ -5 & 13 & -8 \\ 0 & -8 & 8 \end{bmatrix} \tag{2.2}$$

We now study some of the properties of the Laplacian matrix (2.2) which will be generalized later. Its three eigenvalues are non-negative, being $\lambda_1 = 0$, $\lambda_2 = 6$, $\lambda_3 = 20$. The eigenvector relative to λ_1 is $\mathbb{1}$, as we can

see from

$$L\,\mathbb{1} = \begin{bmatrix} 5 & -5 & 0 \\ -5 & 13 & -8 \\ 0 & -8 & 8 \end{bmatrix} \begin{bmatrix} 1 \\ 1 \\ 1 \end{bmatrix} = \begin{bmatrix} 0 \\ 0 \\ 0 \end{bmatrix} = 0\,\mathbb{1}\ .$$

In other words, each row of the matrix sums to zero. Let us now consider the principal sub-block

$$L_{11} = \begin{bmatrix} 5 & -5 \\ -5 & 13 \end{bmatrix}$$

Its eigenvalues are positive, being $\lambda_1 \simeq 2.6$ and $\lambda_2 \simeq 15.4$. Also, the inverse of this sub-block is a *positive* matrix, meaning that all its entries are positive:

$$L_{11}^{-1} = \begin{bmatrix} 0.325 & 0.125 \\ 0.125 & 0.125 \end{bmatrix}$$

These results extend to a generic Laplacian matrix of an undirected weighted graph. It has one zero eigenvalue, whose relative eigenvector is $\mathbb{1}$. The other eigenvalues have positive real part [15, Section 6.13]. Hence the matrix is *positive semi-definite*. Any of its principal sub-blocks is positive definite and therefore invertible. Its inverse is not only a positive definite matrix, but also a positive matrix, meaning that all its entries are positive [16, Corollary 6.2.27]. We do not report here the proof of these facts, as it goes beyond the scope of this Chapter.

The implicit function theorem

The last mathematical tool that we introduce is the *implicit function theorem*. This will be fundamental in the proofs of our two main results, Theorem 3.1 and Theorem 4.1, presented respectively in Chapters 3 and 4. The implicit function theorem is of central importance in the study of nonlinear multivariate functions. It is a local, nonlinear extension of a simple linear algebra result. Namely, if we have a linear system of

equations

$$0 = Cx + Dy \ , \tag{2.3}$$

where $x \in \mathbb{R}^n$, $y \in \mathbb{R}^m$, C is an $m \times n$ matrix and D is an $m \times m$ matrix, then one can solve for y as a function of x if D is invertible. The solution is $y = -D^{-1}Cx$. The implicit function theorem generalizes this fact.

Theorem 2.1 (Implicit function theorem). *Let $f : \mathbb{R}^{n+m} \to \mathbb{R}^m$ be a continuously differentiable function, and let $\mathbb{R}^{n+m}$ have coordinates (x, y), with $x \in \mathbb{R}^n$, $y \in \mathbb{R}^m$. Let the point $(a, b) \in \mathbb{R}^{n+m}$ be such that $f(a, b) = \mathbf{0}$. If the matrix*

$$\frac{\partial f}{\partial y}(a, b) := \left[\frac{\partial f_i}{\partial y_j}(a, b)\right]_{i,j=1}^{m} \tag{2.4}$$

is invertible, then there exists an open set $U \subset \mathbb{R}^n$ containing a, an open set $V \subset \mathbb{R}^m$ containing b, and a unique continuously differentiable function $g : U \to V$ such that

$$f(x, g(x)) = 0 \quad \forall\ x \in U \tag{2.5}$$

Moreover, inside U the expression of the derivative of g with respect to x is given by

$$\frac{\partial g}{\partial x} = -\left\{\frac{\partial f}{\partial y}(x, g(x))\right\}^{-1} \frac{\partial f}{\partial x}(x, g(x)) \tag{2.6}$$

We do not report the proof of the theorem; a thorough treatment can be found in [17, Paragraph 2.5].

2.2 The power grid model

We model a power grid in steady state sinusoidal regime as an unweighted directed graph $\mathcal{G}(\mathcal{V}, \mathcal{E})$, whose nodes (or *buses*) represent loads and sources, and edges represent power lines. The direction of the edges is used as a

reference for the current flow. We assume that the signals are isofrequential. We describe the network dynamics by means of the *phasors* formalism, where each sinusoidal signal can be expressed as a complex number

$$y = |y|e^{j\angle y} \ .$$

The magnitude $|y|$ is the amplitude of the sinusoid and $\angle y$ is the phase shift with respect to a global reference phase. This representation is used for both voltages and currents.
The following variables describe the state of a grid with n nodes and m edges:

- $U \in \mathbb{C}^n$, where U_k is the phasor representation of the voltage at node k;
- $I \in \mathbb{C}^n$, where I_k is the phasor representation of the current injected by node k;
- $\xi \in \mathbb{C}^m$, where ξ_h is the phasor representation of the current flowing on the edge h, whose sign is referred to the direction of the edge.

We denote with B the $m \times n$ incidence matrix of the graph and with Z the $m \times m$ complex diagonal matrix whose element $[Z]_{hh}$ is the impedance of edge h. Then Ohm's law and Kirchhoff's current law can be expressed in vector notation as

$$BU = Z\xi \tag{2.7}$$

$$B^T\xi = I \ . \tag{2.8}$$

Since Z is invertible, we can substitute (2.7) into (2.8) obtaining

$$I = B^T Z^{-1} Bu = YU \ , \tag{2.9}$$

where we introduced the *admittance matrix* $Y := B^T Z^{-1} B$ of the grid. We remind that the *admittance* of a line is the inverse of its impedance. One can verify that the off-diagonal element $[Y]_{ij}$ is equal to the admit-

tance between node i and node j (which is zero if the two nodes are not connected); the diagonal element $[Y]_{ii}$ is equal to the sum of the admittances between node i and any other node.
The node k injects into the grid the complex power

$$S_k = U_k I_k^* \qquad k \in \mathcal{V}. \tag{2.10}$$

Writing $S_k = P_k + jQ_k$, the real part $P_k \in \mathbb{R}$ is the *active power* and the imaginary part $Q_k \in \mathbb{R}$ is the *reactive power*. Combining (2.9) and (2.10) in vector notation, we can express the powers as functions of the voltages:

$$S = P + jQ = \mathrm{diag}(U)(YU)^*\,, \tag{2.11}$$

If we write the complex voltage U_i as $E_i e^{j\phi_i}$ we can reduce (2.11) in components as

$$\begin{aligned} P_i = &\sum\nolimits_{j=1}^{n} \mathfrak{Im}([Y]_{ij}) E_i E_j \sin(\theta_i - \theta_j) \\ &+ \sum\nolimits_{j=1}^{n} \mathfrak{Re}([Y]_{ij}) E_i E_j \cos(\theta_i - \theta_j)\,, \qquad i \in \mathcal{V}\,, \end{aligned} \tag{2.12}$$

and

$$\begin{aligned} Q_i = &-\sum\nolimits_{j=1}^{n} \mathfrak{Im}([Y]_{ij}) E_i E_j \cos(\theta_i - \theta_j) \\ &+ \sum\nolimits_{j=1}^{n} \mathfrak{Re}([Y]_{ij}) E_i E_j \sin(\theta_i - \theta_j)\,, \qquad i \in \mathcal{V}. \end{aligned} \tag{2.13}$$

During regular power system operation the solutions to (2.11) usually [9, 10] satisfy $|\theta_i - \theta_j| \ll 1$ for each $(i,j) \in \mathcal{E}$. We assume from now on that $\theta_i = \theta_j$ for each $(i,j) \in \mathcal{E}$. Under this condition, the reactive power flow equations (2.13) can be written in compact vector notation as

$$Q = \mathrm{diag}(E) L E\,, \tag{2.14}$$

where $L := -\mathfrak{Im}(Y)$. We remind that the imaginary part of the admittance is called *susceptance*. Looking back at the definition of Y in (2.9) and naming $B_{ij} := \mathfrak{Im}(Y_{ij})$ the susceptance between node i and node j,

the expression of L is given by

$$[L]_{ij} = \begin{cases} B_{ij} & \text{for } i \neq j \\ \sum_{k \neq i} -B_{ik} & \text{for } i = j \end{cases}$$

In the rest of the work we will consider power networks in which the inductive component is bigger than the reactive one, so the scusceptance of each line is negative. This implies that the diagonal terms of L are positive and the off-diagonal ones are non-positive. Looking back at the expression of the Laplacian matrix (2.1), we can interpret L as the Laplacian matrix of a new graph $\tilde{\mathcal{G}}$. The graph $\tilde{\mathcal{G}}$ has the same node set $\mathcal{V}$ of the original graph $\mathcal{G}$. Its edge set $\tilde{\mathcal{E}}$ is the undirected version of the edge set $\mathcal{E}$, namely $(i,j) \in \mathcal{E} \Rightarrow (i,j),(j,i) \in \tilde{\mathcal{E}}$. The graph $\tilde{\mathcal{G}}$ is undirected and equipped with a weight function W associating each edge to its susceptance. The analysis of equation (2.14) is of central importance for the rest of the work and we will make use of the properties of the Laplacian matrix L that we introduced in Section 2.1.

Finally, as standard in load flow studies and power system stability analysis, we model loads as stiff constant-reactive power demands [9]. We assume the loads to be of inductive nature, so the reactive power that they inject in the network is negative.

Chapter 3

Approximate solution to the reactive power flow

In this section we partition the network nodes as $\mathcal{V} = \{\mathcal{V}_L, \mathcal{V}_S\}$ corresponding to loads and sources (or generators). We require that the voltage magnitudes at the sources are regulated to constant and predetermined values. We remind that we model the loads as stiff negative constant-reactive power demands. The typical example of such a network is a transmission-level grid consisting of loads and generation sources such as synchronous generators. The voltage magnitude vector and the Laplacian L inherit the partitioning as

$$E = \begin{bmatrix} E_L \\ E_S \end{bmatrix}, \qquad L = \begin{bmatrix} L_{LL} & L_{LS} \\ L_{SL} & L_{SS} \end{bmatrix}.$$

With this in mind, equation (2.14) becomes

$$\begin{bmatrix} Q_L \\ Q_S \end{bmatrix} = \operatorname{diag}(E_L, E_S) \begin{bmatrix} L_{LL} & L_{LS} \\ L_{SL} & L_{SS} \end{bmatrix} \begin{bmatrix} E_L \\ E_S \end{bmatrix}. \tag{3.1}$$

We assume that the source voltages E_S are fixed and no constraints are imposed on the sources power injections Q_S, that is, the sources are PE-buses [9]. Hence, the second block of equations in (3.1) can be thought of as determining Q_S as a function of the load voltages E_L. Thus, equations

(3.1) reduce to their first block:

$$Q_L = \operatorname{diag}(E_L) \begin{bmatrix} L_{LL} & L_{LS} \end{bmatrix} \begin{bmatrix} E_L \\ E_S \end{bmatrix}. \tag{3.2}$$

The variables in these $|\mathcal{V}_L|$ equations (3.2) are the $|\mathcal{V}_L|$ load voltages E_L. In other words, these equations, if solvable, determine E_L as a function of the remaining constant source voltages and network parameters. We point out that $Q_L \leq \mathbf{0}$, because we model loads as stiff constant-reactive power demands.

In general the system of quadratic equations (3.2) is not solvable analytically. The classic example of a two node network nicely illuminates some of the general features of these equations and motivates our subsequent approximation.

Example 3.1 (Two node network). Consider a network with two nodes connected through an inductive line with susceptance $-\ell$. One node is a load with reactive power demand q, while the other node is a source with fixed voltage magnitude $E_N > 0$. Denoting by e the voltage magnitude at the load, (3.2) reduces to

$$q = \ell e(e - E_N). \tag{3.3}$$

If

$$q \geq -q_{\text{crit}} := -\frac{1}{4}\ell E_N^2, \tag{3.4}$$

then equation (3.3) admits two real-valued solutions, given by

$$e_{1,2} = E_N \left(\frac{1}{2} \pm \frac{1}{2}\sqrt{1 + \frac{q}{q_{\text{crit}}}} \right).$$

If $|q/q_{\text{crit}}| \ll 1$, the Taylor expansion ($\sqrt{1+x} \simeq 1 + \frac{1}{2}x$) leads to the approximate expressions:

$$e_1 \simeq E_N + \frac{q}{\ell E_N}, \quad e_2 \simeq -\frac{q}{\ell E_N}. \tag{3.5}$$

The solution e_1 is the desired one in practice, as it corresponds to a high-voltage low-current configuration for the network, resulting in low power losses. In particular, the solution can be interpreted as being roughly E_N, with a correction term linear in the power demand, scaled inversely by both E_N and the line susceptance. □

3.1 Solution and bound on the error term

We now build further on the motivation of Example 3.1 and offer some intuitive derivations on how to generalize the example. We set $E_N := \min_{i\in\mathcal{V}_S} E_i$ and define the vector η so that the voltages can be decomposed into $E = E_N(\mathbb{1} + \eta)$. As in the example, we are interested in the high-voltage solution to the power flow equations and, moreover, we are interested in solutions with uniform voltages. High and uniform voltages correspond to the regime where $E_N \gg 1$ and $\eta \ll 1$. In this regime, equation (3.2) becomes

$$\begin{aligned} Q_L &= E_N \operatorname{diag}(\mathbb{1} + \eta_L) \begin{bmatrix} L_{LL} & L_{LS} \end{bmatrix} E_N(\mathbb{1} + \eta) \\ &= E_N^2 \Big(\begin{bmatrix} L_{LL} & L_{LS} \end{bmatrix} \eta + \operatorname{diag}(\eta_L) \begin{bmatrix} L_{LL} & L_{LS} \end{bmatrix} \eta \Big) \\ &\simeq E_N^2 (L_{LL}\eta_L + L_{LS}\eta_S) \ , \end{aligned} \tag{3.6}$$

where the second equality holds because $\mathbb{1}$ is in the kernel of L, and the last approximation neglects the quadratic term in η. Solving (3.6) for η_L, we obtain the following approximate solution

$$\begin{aligned} E_L &= E_N(\mathbb{1} + \eta_L) \\ &\simeq E_N\mathbb{1} - E_N L_{LL}^{-1} L_{LS}\eta_S + \frac{1}{E_N} L_{LL}^{-1} Q_L \, . \end{aligned} \tag{3.7}$$

Looking back at Example II.1, we see how the first order expansion that led to the solution e_1 in equation (3.5) corresponds exactly to the ap-

proximation (3.7). Building on this intuitive derivations, we now present our first rigorous result, which extends the work carried out in [1] to networks with multiple generating sources. The proof of the following theorem takes inspiration but deviates from the proof strategy in [1]; it uses arguments of multivariate analysis along with the implicit function theorem. We first present a technical Lemma needed for the following proof.

Lemma 3.1 If $\eta_S \geq 0$ the matrix

$$\text{diag}(\mathbb{1} - L_{LL}^{-1} L_{LS} \eta_S) \tag{3.8}$$

is invertible.

Proof The invertibility of (3.8) is equivalent to the fact that each component of the vector $\mathbb{1} - L_{LL}^{-1} L_{LS} \eta_S$ is different from zero. Since L_{LL} is a principal sub-block of a Laplacian matrix, its inverse is a positive matrix (see Section 2.1). Also, the entries of L_{LS} are off-diagonal elements of the Laplacian L, so they are non-positive. These two facts are sufficient to show that $L_{LL}^{-1} L_{LS} \eta_S \leq 0$, which leads to the thesis. □

Theorem 3.1 (Approximate solution to the RPFE). *Consider the reactive power balance equations* (3.2)*, define* $E_N := \min_{i \in \mathcal{V}_S} E_i$ *as the* source baseline voltage*, and let the* source voltage spread η_S *be such that* $E_S = E_N(\mathbb{1} + \eta_S)$*. Define the* approximate load voltage

$$E_{L,\text{approx}} := E_N(\mathbb{1} - L_{LL}^{-1} L_{LS} \eta_S) + \frac{1}{E_N} \left(L_{LL}^{-1} diag^{-1}(\mathbb{1} - L_{LL}^{-1} L_{LS} \eta_S) Q_L \right).$$

Then there exists a minimum voltage $E_N^{\min}$ *such that, for all* $E_N > E_N^{\min}$*, a high-voltage solution of equation* (3.2) *exists and is given by*

$$E_L = E_{L,\text{approx}} + \frac{1}{E_N^3} k\,, \tag{3.9}$$

where the term k satisfies

$$\|k\|_2 \leq \gamma\,, \tag{3.10}$$

being γ only dependent on the network parameters.

Proof To streamline the presentation, we break the proof into the following two parts:

1. existence of the solution (3.9)
2. bound (3.10) on the error term

Part 1 (existence of the solution (3.9)**)**
We first define $\varepsilon = \frac{1}{E_N}$. We perform the change of variables:

$$E_L = \frac{1}{\varepsilon}(\mathbb{1} - L_{LL}^{-1}L_{LS}\eta_S) + \varepsilon\big(L_{LL}^{-1}\mathrm{diag}^{-1}(\mathbb{1} - L_{LL}^{-1}L_{LS}\eta_S)Q_L\big) + \varepsilon\, h\,, \tag{3.11}$$

where we expressed the old variables E_L in terms of the new variables h. In equation (3.2) we rewrite the entire vector $\begin{bmatrix} E_L \\ E_S \end{bmatrix}$ in terms of the new variables:

$$\begin{bmatrix} E_L \\ E_S \end{bmatrix} = \frac{1}{\varepsilon}\begin{bmatrix} \mathbb{1} \\ \mathbb{1} \end{bmatrix} + \frac{1}{\varepsilon}\begin{bmatrix} -L_{LL}^{-1}L_{LS} \\ I \end{bmatrix}\eta_S + \varepsilon\begin{bmatrix} L_{LL}^{-1}\mathrm{diag}^{-1}(\mathbb{1} - L_{LL}^{-1}L_{LS}\eta_S)Q_L + h \\ \mathbf{0} \end{bmatrix} \tag{3.12}$$

We can now compute

$$\begin{bmatrix} L_{LL} & L_{LS} \end{bmatrix}\begin{bmatrix} E_L \\ E_S \end{bmatrix} = \varepsilon L_{LL}\big(L_{LL}^{-1}\mathrm{diag}^{-1}(\mathbb{1} - L_{LL}^{-1}L_{LS}\eta_S)Q_L + h\big)\,, \tag{3.13}$$

where we used the fact that $\mathbb{1}$ is an eigenvector of L relative to 0 and that

$$\begin{bmatrix} L_{LL} & L_{LS} \end{bmatrix}\begin{bmatrix} -L_{LL}^{-1}L_{LS} \\ I \end{bmatrix} = \mathbf{0}$$

Inserting the simplification (3.13) we can rewrite equation (3.2) as

$$\begin{aligned} Q_L &= \operatorname{diag}\Big(\frac{1}{\varepsilon}\Big(\mathbb{1} - L_{LL}^{-1}L_{LS}\eta_S\Big) + \varepsilon\Big(L_{LL}^{-1}\operatorname{diag}^{-1}(\mathbb{1} - L_{LL}^{-1}L_{LS}\eta_S)Q_L + h\Big)\Big) \\ &\quad \cdot \varepsilon L_{LL}\Big(L_{LL}^{-1}\operatorname{diag}^{-1}(\mathbb{1} - L_{LL}^{-1}L_{LS}\,\eta_S)Q_L + h\Big) \\ &= Q_L + \operatorname{diag}(\mathbb{1} - L_{LL}^{-1}L_{LS}\,\eta_S)L_{LL}h + \varepsilon^2 r(h)\,, \end{aligned} \tag{3.14}$$

where we defined the function

$$\begin{aligned} r(h) = &\operatorname{diag}\Big(L_{LL}^{-1}\operatorname{diag}^{-1}(\mathbb{1} - L_{LL}^{-1}L_{LS}\eta_S)Q_L + h\Big) \\ &\cdot L_{LL}\Big(L_{LL}^{-1}\operatorname{diag}^{-1}(\mathbb{1} - L_{LL}^{-1}L_{LS}\,\eta_S)Q_L + h\Big)\,, \end{aligned}$$

which is quadratic in the entries of the vector h. Equation (3.14) can be expressed as

$$\mathbf{0} = \operatorname{diag}(\mathbb{1} - L_{LL}^{-1}L_{LS}\,\eta_S)L_{LL}h + \varepsilon^2 r(h)\,. \tag{3.15}$$

We define the function

$$f(\varepsilon, h) = \operatorname{diag}(\mathbb{1} - L_{LL}^{-1}L_{LS}\,\eta_S)L_{LL}h + \varepsilon^2 r(h)\,,$$

so we can rewrite the right-hand side of (3.15) as

$$\mathbf{0} = f(\varepsilon, h)\,. \tag{3.16}$$

We want to apply the implicit function theorem (see Section 2.1) on the function f. This is in fact a polynomial function in its variables, hence it is continuously differentiable. The point $(0, \mathbf{0})$ solves equation (3.15):

$$\mathbf{0} = f(0, \mathbf{0}) \tag{3.17}$$

Let us compute

$$\left[\frac{\partial f_i}{\partial h_j}(0, \mathbf{0})\right] = \operatorname{diag}(\mathbb{1} - L_{LL}^{-1}L_{LS}\,\eta_S)L_{LL} \tag{3.18}$$

which is invertible (see Lemma 3.1). The implicit function theorem ensures the existence of the open sets $U_0 \subset \mathbb{R}$, $V_{\mathbf{0}} \subset \mathbb{R}^{|\mathcal{V}_L|}$ (containing the respective origins) and of a continuously differentiable function

$$\begin{aligned} H : U_0 &\to V_{\mathbf{0}} \\ \varepsilon &\mapsto h = H(\varepsilon)\,. \end{aligned}$$

The function H is such that

$$\mathbf{0} = f(\varepsilon, H(\varepsilon))\,, \qquad \text{for } \varepsilon \in U_0\,. \tag{3.19}$$

Define now $k := E_N^2\, h$. The fact that for $\varepsilon \in U_0$ there exists h for which the equation (3.15) is satisfied, implies the existence of $E_N^{\min}$ such that, for $E_N > E_N^{\min}$ there exists a solution to the equation (3.2) of the form (3.9).

Part 2 (bound (3.10) **on the error term)**
From the continuity of the function H it follows that

$$\lim_{\varepsilon \to 0} H(\varepsilon) = \mathbf{0}$$

which is equivalent to

$$\lim_{E_N \to \infty} h = \mathbf{0} \tag{3.20}$$

From equation (3.15) we can write the following equality between 2-norms

$$\left\| \mathrm{diag}(\mathbb{1} - L_{LL}^{-1} L_{LS}\, \eta_S) L_{LL} h \right\|_2 = \varepsilon^2 \left\| r(h) \right\|_2 \tag{3.21}$$

The entries of the vector $r(h)$ are polynomials of degree 2 in the entries of the vector h. By means of a series of elementary inequalities on the 2-norm it can be shown that there exists a real number β such that

$$\|r(h)\| \leq \beta (1 + \|h\|)^2 \tag{3.22}$$

We now find a lower bound on the left-hand side of equation (3.21). First, we remind that $\mathrm{diag}(\mathbb{1} - L_{LL}^{-1} L_{LS}\, \eta_S)$ is a diagonal elements with positive diagonal; we define $\alpha_1 := \min_{i \in S} \mathbb{1} - L_{LL}^{-1} L_{LS}\, \eta_S$. Then we remind that

all the eigenvalues of L_{LL} are positive; we define the minimum eigenvalue of L_{LL} as α_2. We can now express the lower bound as

$$\alpha \|h\| := \alpha_1 \alpha_2 \|h\| \leq \left\| \mathrm{diag}(\mathbb{1} - L_{LL}^{-1} L_{LS}\, \eta_S) L_{LL} h \right\|_2 \tag{3.23}$$

Combining equality (3.21) and inequalities (3.22) and (3.23) we obtain

$$\frac{\alpha}{\beta} E_N^2 \|h\| \leq (1 + \|h\|)^2 \tag{3.24}$$

It can be proved that inequality (3.24) implies that one of the two following inequalities holds

$$\|h\| \leq \frac{4\beta}{\alpha E_N^2} \qquad \text{or} \qquad \|h\| \geq \frac{\alpha}{\beta} E_N^2 - 2 - \frac{4\beta}{\alpha E_N^2}$$

The limit (3.20) excludes the second possibility, so we are left with

$$\|h\| \leq \frac{4\beta}{\alpha E_N^2} := \frac{\gamma}{E_N^2}\,,$$

which, reminding that $k := E_N^2\, h$, implies the thesis (3.10). □

3.2 Approximation and asymptotic behavior of the error term

The first result that Theorem 3.1 provides is that above a threshold $E_N^{\min}$ the existence of a a solution to the reactive power flow equations is guaranteed. This is true in particular for the two node grid studied in Example 3.1, where the condition for the existence of real-valued solution (3.4) can be rewritten as

$$E_N \geq \sqrt{\frac{-4q}{\ell}}\,.$$

So in the two node case the threshold $E_N^{\min}$ is $\sqrt{-4q/\ell}$. In the numerical study case we will find the value of the threshold through simulation of

a more complex network.

Equation (3.9) tells us that that as the source baseline E_N becomes large and the source voltage spread η_S diminishes, the load voltage solution tends to the source baseline E_N. Indeed, this regime is the practically relevant case occurring in regular power system operation, and this qualitative behavior of the error term agrees with classic power systems intuition [7].

The bound (3.10) on k allows us to derive from equation (3.9) an approximate solution to the reactive power flow equations:

$$E_L \simeq E_N(\mathbb{1} - L_{LL}^{-1}L_{LS}\eta_S) + \frac{1}{E_N}\left(L_{LL}^{-1}\mathrm{diag}^{-1}(\mathbb{1} - L_{LL}^{-1}L_{LS}\eta_S)Q_L\right), \quad (3.25)$$

where we discarded the *error term* $\frac{1}{E_N^3}\,k$, which we denote as $\delta(E_N)$. We remark that expression (3.25) is the *approximate solution* to the reactive power flow equations.
The bound gives information on the asymptotic behavior of δ, namely:

$$\limsup_{E_N \to \infty} \frac{\delta(E_N)}{\frac{1}{E_N^3}} = \text{const} \in \mathbb{R}\,. \quad (3.26)$$

In words, the error term δ goes to zero at least as fast as $\frac{1}{E_N^3}$. We can study the behavior of the error term in the two node grid. In Example 3.1 we utilized the Taylor expansion $\sqrt{1+x} \simeq 1 + \frac{x}{2}$ to find the approximate solution reported in equation (3.5); if we compute also the third term of the expansion ($\sqrt{1+x} \simeq 1 + \frac{x}{2} - \frac{x^2}{8}$) we can write the *exact* solution as

$$E_N + \frac{q}{\ell E_N} - \frac{q^2}{\ell^2 E_N^3} + o\left(\frac{1}{E_N^3}\right), \quad (3.27)$$

where, with abuse of notation, we indicate with the symbol $o(1/E_N^3)$ a generic function belonging to the set $o(1/E_N^3)$. Equation (3.25) gives us

the approximate solution

$$E_N + \frac{q}{\ell E_N}\,. \tag{3.28}$$

Comparing (3.27) and (3.28) we deduce that the expression of the error term in the two node grid is

$$\delta = -\frac{q^2}{\ell^2 E_N^3} + o\left(\frac{1}{E_N^3}\right). \tag{3.29}$$

When E_N goes to infinity, (3.29) tends to zero exactly as $\frac{1}{E_N^3}$, in accordance with the bound (3.10) provided by Theorem 3.1.
The Taylor expansion of the square root reveals that the exact expression (3.27) is an expansion in odd powers of E_N (with exponents 1, -1, -3, -5 and so on). We expect the generic solution of the reactive power flow equations (3.2) to present the same kind of expansion, and Theorem 3.1 partially shows this, basically proving that the expansion holds for the exponents 1, -1 and -3. In the numerical study case we will show that the odd series continues also with the exponent -5.

3.3 Comparison of the two approximations

The goal of this paragraph is to analyze the relationship between the rigorous approximation derived by Theorem 3.1

$$E_L \simeq E_N(\mathbb{1} - L_{LL}^{-1}L_{LS}\eta_S) + \frac{1}{E_N}\left(L_{LL}^{-1}\mathrm{diag}^{-1}(\mathbb{1} - L_{LL}^{-1}L_{LS}\eta_S)Q_L\right), \tag{3.25}$$

and the intuitive approximation proposed by equation (3.7)

$$E_L \simeq E_N\mathbb{1} - E_N L_{LL}^{-1}L_{LS}\eta_S + \frac{1}{E_N}L_{LL}^{-1}Q_L\,. \tag{3.7}$$

We number the rigorous approximation as 1 and the intuitive approximation as 2. The reason for which we are interested in the approximation

2 is that it is the extension of part of the work presented in [1]. The difference between the two approximations is the presence of the term

$$D := -L_{LL}^{-1} L_{LS} \eta_S \,. \tag{3.30}$$

To understand its role, we investigate again the two node grid. If we set $\eta = 0$ as we did in Example 3.1 then the difference term D disappears and the two approximations coincide. For this reason, we set the fixed source voltage at the value $E_S = E_N(1 + \eta_S)$, with $\eta_S > 0$. Decoupling the source baseline voltage and the source voltage spread, even though is not very meaningful in the two node grid, helps the understanding of the role of the difference term D. Computing the expressions of the approximations 1 and 2 in the two node example gives

$$E_{L,\text{approx},1} = E_S + \frac{q}{\ell E_S} \,, \tag{3.31}$$

$$E_{L,\text{approx},2} = E_S + \frac{q}{\ell E_N} \,. \tag{3.32}$$

Reminding that the exact solution is

$$E_S + \frac{q}{\ell E_S} - \frac{q^2}{\ell^2 E_S^3} + o\left(\frac{1}{E_N}^3\right), \tag{3.33}$$

we see that intuitive approximation fails to fully characterize the term of order $\frac{1}{E_N}$, while the rigorous is able to do it. This is due to the presence of the difference term D, which takes into account the source voltage spread η_S. On the contrary, the intuitive approximation does not take into account the source voltage spread when characterizing the term of order $\frac{1}{E_N}$. For this reason we expect the approximation error $\delta_2(E_N)$ resulting from approximation 2 to tend to zero as $1/E_N$. This asymptotic behavior can be expressed as

$$\lim_{E_N \to \infty} \frac{\delta_2(E_N)}{\frac{1}{E_N}} = \text{const} \neq 0 \tag{3.34}$$

We can study the difference D in terms of the sign of its contribution to approximation 1:

$$E_{L,\text{approx},1} \geq E_{L,\text{approx},2} \ , \tag{3.35}$$

because

$$L_{LL}^{-1}\,\text{diag}^{-1}(\mathbb{1} - L_{LL}^{-1}L_{LS}\eta_S)\,Q_L > L_{LL}^{-1}\,Q_L \,. \tag{3.36}$$

Inequality (3.36) holds because L_{LL}^{-1} and η_S are positive, L_{LS} and Q_L are negative. The interpretation for this inequality is the following: since the difference term takes into account that the source voltage is higher than the baseline E_N (it takes it into account by incorporating η_S), in its solution the load voltage drops less than what it drops in the intuitive approximation, where the information about η_S is not exploited. It is as if the approximation 1 sees the source voltage as lower than what it really is, hence letting drop the load voltage in order to provide the same amount of reactive power.
Inequality (3.35) along with its interpretation suggest than relying on approximation 1 leads to a more conservative network design than relying on approximation 2, which is therefore more valuable for practical purposes

3.4 Numerical case study of the approximate solution

In this section we test the results obtained in Theorem 3.1 on the standard IEEE 37 distribution network, which we report in Figure 3.1.

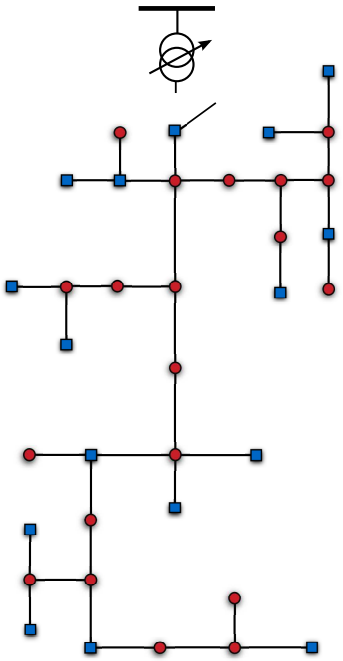

Figure 3.1: Islanded IEEE 37 bus distribution network containing loads ● and inverters ■

The nominal operating voltage of this monophase network is 4.8 kV. The line susceptances vary in the range $[-0.5\ \text{H}, -10\ \text{H}]$ with R/X ratios of approximately one, while the reactive power demands vary for each load in the interval $[-30\ \text{kvar}, -70\ \text{kvar}]$. The sources voltage magnitudes are fixed values in the interval $[E_N, E_N + 0.1\, E_N]$. We decouple the power flow equations and analyze numerically the resulting reactive load flow equations (3.2) for different values of the baseline source voltage E_N. In particular we study:

a) The threshold $\tilde{E}_N^{\min}$ above which the solution (3.9) exists.
b) The accuracy of its approximate expression. We consider both the approximations that we presented, namely approximation 1 (equa-

tion (3.25)) and approximation 2 (equation (3.7)). To quantify the error between the numerical solution of the nonlinear reactive load flow equations and the approximations 1 and 2, we introduce the *relative approximation errors*

$$r_i := \frac{\|\delta_i(E_N)\|_\infty}{E_N} = \frac{\|E_{\mathrm{L,nonlin}} - E_{\mathrm{L,approx,i}}\|_\infty}{E_N}\,, \quad i \in \{1,2\}\,.$$

The threshold $\tilde{E}_N^{\min}$ above which the high-voltage solution exists was found by simulation to be roughly 370V, well below the muli-kV range in which the system is operated.

Figure 3.2 reports the relative approximation errors r_1 and r_2 for the approximations 1 and 2 in the IEEE 37 network, for different values of E_N. Both the axis are reported in logarithmic scale.

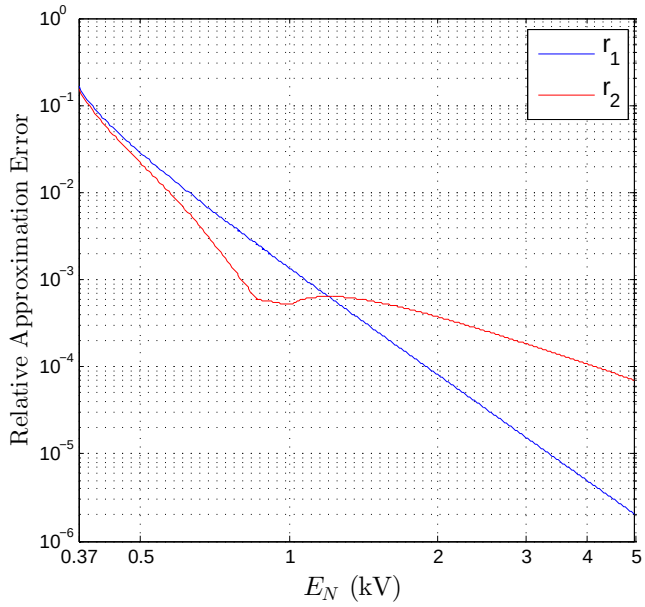

Figure 3.2: The log-log plot of the relative errors of approximation 1 and 2, computed numerically for different values of the baseline source voltage E_N. The threshold $E_N^{min} = 370$V is marked.

Note first that both relative approximation errors decrease rapidly as $\tilde{E}_N$ grows. In particular at the 4.8kV nominal operating voltage of the network, the relative error using both approximations is below 0.1%, with the accuracy of approximation 1 being below 0.01%.
In Figure 3.3 for each E_N we report $\delta_1(E_N)\cdot E_N^3$ and $\delta_2(E_N)\cdot E_N$. The fact that the two curves tend to a constant value shows that the approximation error δ_1 tends to zero exactly as $1/E_N^3$ and the approximation error δ_2 tends to zero exactly as $1/E_N$. This corresponds to what we proved in equation (3.26) and in equation (3.34).

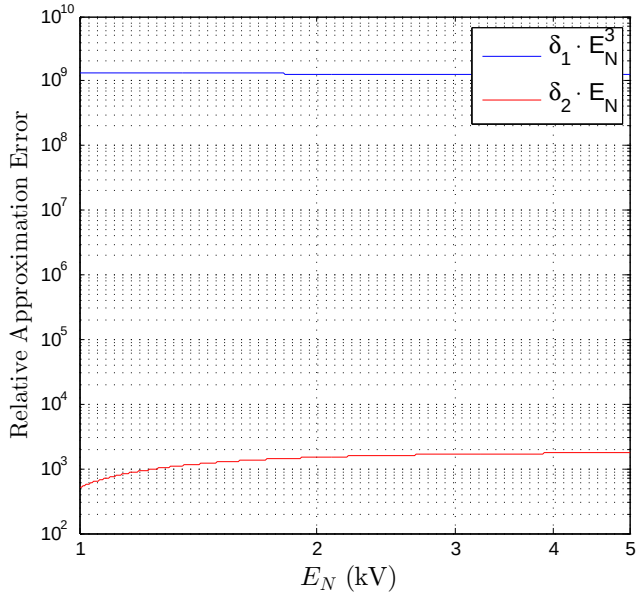

Figure 3.3: The log-log plot of the errors scaled by appropriate powers of E_N shows the asymptotic behavior of the errors.

Chapter 4

Application to the droop control for voltage stabilization

In this section, we consider the problem of voltage stabilization in an inverter-based microgrid. We partition the set of nodes in the microgrid as $\mathcal{V} = \{\mathcal{V}_L, \mathcal{V}_I\}$, where $\mathcal{V}_L$ are loads and $\mathcal{V}_I$ are inverters. The reactive load flow equation (3.2) can be rewritten as

$$Q_L = \operatorname{diag}(E_L) \begin{bmatrix} L_{LL} & L_{LI} \end{bmatrix} \begin{bmatrix} E_L \\ E_I \end{bmatrix}. \tag{4.1}$$

4.1 Quadratic droop control and its network interpretation

The power injections at the inverters are governed by the *quadratic droop controller* [14]. This recently proposed controller adjusts the inverter voltage magnitude according to

$$\tau_i \dot{E}_i = -C_i E_i (E_i - E_i^R) - Q_i \,, \qquad i \in \mathcal{V}_I \,, \tag{4.2}$$

where $\tau_i, C_i > 0$ are fixed controller parameters, and E_i^R is a fixed *reference voltage*. The quantity E_I^R is referred to as reference voltage because if the inverter i injects no reactive power, the equilibrium voltage of (4.2) is E_i^R.

We make here the important hypothesis that the dynamics of the electrical circuit are considerably faster than the ones of our controllers, so we can assume that the transient of the electrical dynamics is negligible. Equation (4.2) can be expressed in vector notation as

$$\begin{aligned}\tau\dot{E}_I &= C\mathrm{diag}(E_I)(E_R - E_I) - Q_I \\ &= C\mathrm{diag}(E_I)(E_R - E_I) - \mathrm{diag}(E_I)\begin{bmatrix} L_{IL} & L_{II}\end{bmatrix}\begin{bmatrix} E_L \\ E_I\end{bmatrix}, \end{aligned} \tag{4.3}$$

where $\tau = \mathrm{diag}([\tau_i]_{i\in\mathcal{V}_I})$ and $C = \mathrm{diag}([C_i]_{i\in\mathcal{V}_I})$ are diagonal matrices, while $E_R = [E_i^R]_{i\in\mathcal{V}_R}$ is the vector of the reference voltages. By combining the reactive power flow equations at the load (3.2) and the controller (4.3), we obtain the differential-algebraic system

$$\begin{bmatrix}\mathbf{0} \\ \tau\dot{E}_I\end{bmatrix} = \begin{bmatrix} Q_L \\ C\mathrm{diag}(E_I)(E_R - E_I)\end{bmatrix} - \mathrm{diag}(E)LE\ , \tag{4.4}$$

We point out that while in Chapter 3 the voltages E_S were considered to be fixed, now due to the introduction of the quadratic droop controller the voltages E_I in (4.4) are variables of the system; hence the variables are now E_L and E_I. The total number of equations in (4.4) is $|\mathcal{V}_L| + |\mathcal{V}_I|$. The goal of this Chapter is to study whether the differential-algebraic system (4.4) possesses a fixed point, to determine its stability, and find an approximate expression.

We are now going to provide a network interpretation of the quadratic droop controller. In Section 2.2 we saw that in the reactive power flow

equations (2.13) the matrix

$$L = \begin{bmatrix} L_{LL} & L_{LI} \\ L_{IL} & L_{II} \end{bmatrix} \tag{4.5}$$

can be interpreted as the Laplacian matrix of the weighted undirected graph $\tilde{\mathcal{G}}$. The nodes $\mathcal{V}$ of the graph are the loads $\mathcal{V}_L$ and the inverters $\mathcal{V}_I$ of the power grid. The undirected edges $\mathcal{E}$ are the power lines, with the weight of each edge being equal to the reactance of the power line.

Comparing (4.2) and the right-hand side of (3.3), the term $C_i E_i(E_i - E_i^R)$ in (4.2) can be interpreted as the reactive power injected from inverter i to a fictitious node of voltage E_i^R through a line of susceptance $-C_i$. Guided by this intuition, we consider an *extended graph* (or extended network) (Figure 4.1) where we introduce the set of reference nodes $\mathcal{V}_R$ and we connect each node $i \in \mathcal{V}_I$ to the corresponding reference node $i \in \mathcal{V}_R$ through a line of susceptance $-C_i$. The voltage at the new reference node $i \in \mathcal{V}_R$ is fixed at the reference value E_i^R. The voltage vector and Laplacian matrix of the extended network are

$$\tilde{E} = \begin{bmatrix} E_L \\ E_I \\ E_R \end{bmatrix}, \quad \tilde{L} = \begin{bmatrix} L_{LL} & L_{LI} & \mathbf{0} \\ L_{IL} & L_{II} + C & -C \\ \mathbf{0} & -C & C \end{bmatrix}, \tag{4.6}$$

where the diagonal matrix C represents the new connections established between inverters $\mathcal{V}_I$ and reference nodes $\mathcal{V}_R$.

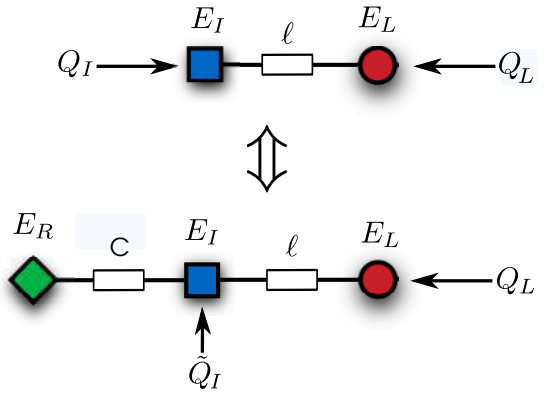

Figure 4.1: The equivalence between the original network (top) which consists of an inverter (blue square) ■ feeding a load ●, and the extended network (bottom) with an additional fictitious node ◆ held at constant voltage E_R.

From (4.6) we can compute the reactive power at the inverters in the extended network, which we denote by $\tilde{Q}_I$:

$$\begin{aligned}\tilde{Q}_I &= \mathrm{diag}(E_I)\begin{bmatrix} L_{IL} & L_{II}+C & -C\end{bmatrix}\tilde{E} \\ &= C\mathrm{diag}(E_I)(E_I - E_R) + Q_I \ ,\end{aligned} \tag{4.7}$$

Using (4.7) the quadratic droop controller (4.3) can now be expressed as

$$\tau \dot{E}_I = -\tilde{Q}_I \ . \tag{4.8}$$

Using (4.8) we can write the differential-algebraic system (4.4) on the extended network equivalently as

$$\begin{bmatrix} Q_L \\ \tilde{Q}_I \end{bmatrix} = \mathrm{diag}(E_L, E_I)\begin{bmatrix} L_{LL} & L_{LI} & \mathbf{0} \\ L_{IL} & L_{II}+C & -C \end{bmatrix}\tilde{E} \tag{4.9a}$$

$$\tau \dot{E}_I = -\tilde{Q}_I \ . \tag{4.9b}$$

We emphasize that (4.9) and (4.4) are equivalent representations of the microgrid with quadratic droop control at the inverters. In particular, the

voltage values at the loads and inverters remain the same in the original and in the extended networks; the only value that changes is the reactive power at the inverters as just explained (the notation captures this change by using $\tilde{Q}_I$ instead of Q_I). Another difference is that the variables of (4.4) are E_L and E_I, while in (4.9) $\tilde{Q}_I$ are also considered as variables.

4.2 Existence and stability of the fixed point

The equations (4.9a) have the same structure as the original load reactive power flow equation (3.2); in Chapter 3 we introduced the approximate solution (3.25) to the original load reactive power flow equation (3.2). We can now follow a similar path and apply the same approximation to equation (4.9a) to find an approximate solution for the voltages E_L and E_I, while E_R is considered to be fixed. We can then use this solution to study the stability of the unique equilibrium $\tilde{Q}_I = \mathbf{0}$ of (4.9b). More precisely, we perform a change of coordinates in equation (4.9), using the approximation errors as the new system variables. In doing so, we facilitate the analysis of the fixed points of the system (4.9).

In order to state our main result, we define the *reference baseline voltage* $\tilde{E}_N$ by

$$\tilde{E}_N := \min_{i \in \mathcal{V}_R} E_i^R,$$

and the *reference voltage spread* $\tilde{\eta}$ such that

$$E_R = \tilde{E}_N(\mathbb{1} + \tilde{\eta}).$$

Note that $\tilde{\eta} \geq \mathbf{0}$. We denote the top-left principal sub-block of the extended Laplacian as

$$\mathcal{L} := \begin{bmatrix} L_{LL} & L_{LI} \\ L_{IL} & L_{II} + C \end{bmatrix}. \tag{4.10}$$

In Section 2.1 we argued how a principal sub-block of a Laplacian matrix is invertible. We define its inverse by

$$X = \begin{bmatrix} X_{LL} & X_{LI} \\ X_{IL} & X_{II} \end{bmatrix} := \begin{bmatrix} L_{LL} & L_{LI} \\ L_{IL} & L_{II} + C \end{bmatrix}^{-1} = \mathcal{L}^{-1}\,, \tag{4.11}$$

and the *hybrid* matrix by

$$M = \begin{bmatrix} M_L \\ M_I \end{bmatrix} := -\begin{bmatrix} L_{LL} & L_{LI} \\ L_{IL} & L_{II} + C \end{bmatrix}^{-1} \begin{bmatrix} \mathbf{0} \\ -C \end{bmatrix},$$

where the name hybrid derives from the fact that this matrix appears in the hybrid current-voltage representation of the grid. We are now ready to state the main result of this section.

Theorem 4.1 (Existence and Stability of the Fixed Point). *There exists a minimum reference baseline voltage $\tilde{E}_N^{\min}$ such that for all $\tilde{E}_N > \tilde{E}_N^{\min}$ the differential-algebraic system (4.4) has a locally exponentially stable high-voltage fixed point given by*

$$\begin{bmatrix} E_L^{eq} \\ E_I^{eq} \end{bmatrix} = \tilde{E}_N(\mathbb{1} + M\tilde{\eta}) + \frac{1}{\tilde{E}_N} \begin{bmatrix} X_{LL} \\ X_{LI} \end{bmatrix} diag^{-1}(\mathbb{1} + M_L\tilde{\eta})Q_L + \frac{1}{\tilde{E}_N^3} k^{\mathrm{eq}}\,, \tag{4.12}$$

where the norm of the term g^{eq} can be bounded as

$$\|k^{\mathrm{eq}}\|_2 \leq \tilde{\gamma}\,, \tag{4.13}$$

with $\tilde{\gamma}$ only depending on the network parameters.

The proof of Theorem 4.1 will take inspiration from Theorem 3.1. At this point, notice that if we insert set $k^{\mathrm{eq}} = \mathbf{0}$ in the expression (4.12), we obtain exactly the approximation (3.25), expressed for the extended network and with $\tilde{Q}_I$ fixed to zero.
However, the two Theorems address two different problems. While Theorem 3.1 focuses on the existence and expression of the solution of the

algebraic equation (3.2), the goal of Theorem 4.1 is to study the existence and the stability of a fixed point of a differential-algebraic system.

Proof To streamline the presentation, we break the proof into the following three parts:

1. change of variables and simplifications;
2. implicit function theorem for large $\tilde{E}_N$;
3. local stability analysis of fixed point;
4. bound (4.13) on the error term

Part 1 (Change of variables and simplifications): Consider the linear change of variables from E_L and E_I to g_L and g_I defined by

$$\begin{bmatrix} E_L \\ E_I \end{bmatrix} = \tilde{E}_N(\mathbb{1} + M\tilde{\eta}) + \frac{1}{\tilde{E}_N} \begin{bmatrix} g_L \\ g_I \end{bmatrix} ,$$

where the old variables E_L, E_I are expressed in terms of the new variables g_L, g_I. Let us define the following quantities and shorthands:

$$\varepsilon := \frac{1}{\tilde{E}_N} \qquad Q := \begin{bmatrix} Q_L \\ \tilde{Q}_I \end{bmatrix} \qquad g := \begin{bmatrix} g_L \\ g_I \end{bmatrix} .$$

Writing the entire voltage vector in terms of the new variables g_L, g_I we obtain

$$\tilde{E} = \begin{bmatrix} E_L \\ E_I \\ E_R \end{bmatrix} = \tilde{E}_N \begin{bmatrix} \mathbb{1} \\ \mathbb{1} \\ \mathbb{1} \end{bmatrix} + \tilde{E}_N \begin{bmatrix} M_L \\ M_I \\ I \end{bmatrix} \tilde{\eta} + \frac{1}{\tilde{E}_N} \begin{bmatrix} g_L \\ g_I \\ \mathbf{0} \end{bmatrix} , \tag{4.14}$$

We now want to insert this expression into the system (4.9). We first notice that

$$\begin{bmatrix} L_{LL} & L_{LI} & \mathbf{0} \\ L_{IL} & L_{II} + C & -C \end{bmatrix} \tilde{E} = \varepsilon \mathcal{L} g , \tag{4.15}$$

Using equality (4.15) we can reformulate the system (4.9) as

$$\begin{aligned} Q &= \left(\frac{1}{\varepsilon}\mathrm{diag}(\mathbb{1} + M\tilde{\eta}) + \varepsilon\ \mathrm{diag}(g)\right)\varepsilon\mathcal{L}g \\ -\tilde{Q}_I &= \frac{d}{dt}\left(\frac{1}{\varepsilon}(\mathbb{1} + M_I\tilde{\eta}) + \varepsilon g_I\right), \end{aligned}$$

where without loss of generality we assumed $\tau = I$. Expanding the first block of the above equations and using the fact that $\tilde{\eta}$ is constant in time we obtain

$$\mathbf{0} = -Q + \mathrm{diag}(\mathbb{1} + M\tilde{\eta})\mathcal{L}g + \varepsilon^2\mathrm{diag}(g)\mathcal{L}g \tag{4.16a}$$

$$-\tilde{Q}_I = \varepsilon X_{II}\dot{\tilde{Q}}_I + \varepsilon\dot{g}_I\ , \tag{4.16b}$$

Part 2 (Implicit function theorem for large $\tilde{E}_N$): If we define the function

$$f(\varepsilon, g, \tilde{Q}_I) := -Q + \mathrm{diag}(\mathbb{1} + M\tilde{\eta})\mathcal{L}g + \varepsilon^2\mathrm{diag}(g)\mathcal{L}g\,, \tag{4.17}$$

then algebraic equation (4.16a) has the form

$$\mathbf{0} = f(\varepsilon, g, \tilde{Q}_I)\ . \tag{4.18}$$

We want to apply the implicit function theorem (see Section 2.1) on the function f. This is in fact a polynomial function in its variables, hence it is continuously differentiable. If we define the value

$$g^{lim} = \mathcal{L}^{-1}\mathrm{diag}^{-1}(\mathbb{1} + M\tilde{\eta})\begin{bmatrix} Q_L \\ \mathbf{0}\end{bmatrix} = \begin{bmatrix} X_{LL} \\ X_{LI}\end{bmatrix}\mathrm{diag}^{-1}(\mathbb{1} + M_L\tilde{\eta})Q_L,$$

it is straightforward to verify that

$$\mathbf{0} = f(\varepsilon = 0, g = g^{lim}, \tilde{Q}_I = \mathbf{0})\,. \tag{4.19}$$

Let us compute

$$\left[\frac{\partial f_i}{\partial g_j}(0, g^{lim}, \mathbf{0})\right] = \mathrm{diag}(\mathbb{1} + M\tilde{\eta})\mathcal{L}\,. \tag{4.20}$$

The matrix $\mathcal{L}$ is invertible, and applying Lemma 3.1 to the extended network guarantees the invertibility of the matrix $\mathrm{diag}(\mathbb{1} + M\tilde{\eta})$. Then their product (4.20) is also invertible. The implicit function theorem ensures the existence of the open sets $U_0 \subset \mathbb{R}$, $W_0 \subset \mathbb{R}^{|\mathcal{V}_I|}$, $V_0 \subset \mathbb{R}^{|\mathcal{V}_I|+|\mathcal{V}_L|}$ (containing the respective origins) and of a continuously differentiable function

$$\begin{aligned} G : U_0 \times W_{\mathbf{0}} &\to V_{\mathbf{0}} \\ (\varepsilon, \tilde{Q}_I) &\mapsto g = G(\varepsilon, \tilde{Q}_I)\,. \end{aligned}$$

The function G is such that

$$\mathbf{0} = f(\varepsilon, \tilde{Q}_I, G(\varepsilon, \tilde{Q}_I))\,, \qquad \text{for } \varepsilon \in U_0\,, \tilde{Q}_I \in W_{\mathbf{0}}\,. \tag{4.21}$$

Substituting $g_I = G_I(\varepsilon, \tilde{Q}_I)$ into the dynamics (4.16b) we obtain

$$-\tilde{Q}_I = \varepsilon\, \dot{G}_I(\varepsilon, \tilde{Q}_I) = \varepsilon\, \frac{\partial G_I}{\partial \tilde{Q}_I}(\varepsilon, \tilde{Q}_I)\dot{\tilde{Q}}_I\ . \tag{4.22}$$

The matrix $\partial G_I / \partial \tilde{Q}_I$ is a sub-matrix of $\partial G / \partial \tilde{Q}_I$, whose expression is provided by the implicit function theorem (see (2.6)) as

$$\frac{\partial G}{\partial \tilde{Q}_I}(\varepsilon, \tilde{Q}_I) = -\left(\frac{\partial f}{\partial g}(\varepsilon, \tilde{Q}_I)\right)^{-1} \frac{\partial f}{\partial \tilde{Q}_I}(\varepsilon, \tilde{Q}_I)\,,$$

which holds in $U_0 \times W_0$ and can be computed as

$$\frac{\partial G}{\partial \tilde{Q}_I} = -\Big(\mathrm{diag}(\mathbb{1} + M\tilde{\eta})\mathcal{L} + \varepsilon^2\big(\mathrm{diag}(g)\mathcal{L} + \mathrm{exdiag}(\mathrm{diag}(g)\mathcal{L})\big)\Big)^{-1} \begin{bmatrix} \mathbf{0} \\ -I \end{bmatrix} \tag{4.23}$$

The matrix $\mathrm{exdiag}(A)$ is defined such that its off-diagonal elements are zero and the its diagonal elements coincide with the diagonal elements of A.

Part 3 (Fixed point and its stability): In $U_0 \times V_0$ we have that $\varepsilon, \tilde{Q}_I$

and $G(\varepsilon, \tilde{Q}_I)$ are bounded. Therefore, from (4.23) we can compute

$$\begin{aligned}\lim_{\varepsilon\to 0} \frac{\partial G}{\partial \tilde{Q}_I} &= \mathcal{L}^{-1}\mathrm{diag}^{-1}(\mathbb{1} + M\tilde{\eta}) \begin{bmatrix} \mathbf{0} \\ -I \end{bmatrix} \\ &= \begin{bmatrix} X_{LL} & X_{LI} \\ X_{IL} & X_{II} \end{bmatrix} \begin{bmatrix} \mathbf{0} \\ \mathrm{diag}^{-1}(\mathbb{1} + M_I\tilde{\eta}) \end{bmatrix} \\ &= \begin{bmatrix} X_{LI} \\ X_{II} \end{bmatrix} \mathrm{diag}^{-1}(\mathbb{1} + M_I\tilde{\eta})\end{aligned}$$

It follows that

$$\lim_{\varepsilon\to 0} \frac{\partial G_I}{\partial \tilde{Q}_I}(\varepsilon, \tilde{Q}_I) = X_{II}\ \mathrm{diag}^{-1}(\mathbb{1} + M_I\eta)\ . \tag{4.24}$$

The right-hand side of (4.24) is invertible. Since the invertibility of the matrix depends continuously on the matrix entries, there exists $\hat{\varepsilon} > 0$ such that for all $\varepsilon < \hat{\varepsilon}$ the matrix

$$\frac{\partial G_I}{\partial \tilde{Q}_I}(\varepsilon, \tilde{Q}_I)\ .$$

is also invertible. Thus, for $\varepsilon < \hat{\varepsilon}$, we can now obtain from (4.22) the explicit dynamical system

$$\dot{\tilde{Q}}_I = -\frac{1}{\varepsilon}\left(\frac{\partial G_I}{\partial \tilde{Q}_I}(\varepsilon, \tilde{Q}_I)\right)^{-1} \tilde{Q}_I \tag{4.25}$$

$$:= A(\tilde{Q}_I)\tilde{Q}_I := \varphi(\tilde{Q}_I)\ , \tag{4.26}$$

where we defined A and φ to keep the notation compact. Observe from (4.25) that $\tilde{Q}_I = \mathbf{0}$ is the unique fixed point of the dynamics. The Jaco-

bian of the system (4.25) around $\tilde{Q}_I = \mathbf{0}$ is given by

$$\left.\frac{\partial \varphi(\tilde{Q}_I)}{\partial \tilde{Q}_I}\right|_{\tilde{Q}_I=0} = A(\tilde{Q}_I = \mathbf{0}) \\ = -\frac{1}{\varepsilon}\left(\frac{\partial G_I}{\partial \tilde{Q}_I}(\varepsilon, \tilde{Q}_I = \mathbf{0})\right)^{-1} . \tag{4.27}$$

Since the inverse of a matrix is continuous with respect to the matrix entries, (4.24) leads to

$$\lim_{\varepsilon\to 0}\left(\frac{\partial G_I}{\partial \tilde{Q}_I}(\varepsilon, \mathbf{0})\right)^{-1} = \left(\lim_{\varepsilon\to 0}\frac{\partial G_I}{\partial \tilde{Q}_I}(\varepsilon, \mathbf{0})\right)^{-1} = \mathrm{diag}(\mathbb{1} + X_{II}C\eta)\ X_{II}^{-1} .$$

The product between a diagonal positive definite matrix and a positive definite matrix has all the eigenvalues with positive real part (see [20] or [21, §6.2]).

As the eigenvalues of a matrix depend continuously on the matrix entries, it is possible to find $\varepsilon^{max} \in]0, \hat{\varepsilon}[$ such that, for all $\varepsilon < \varepsilon^{max}$, the Jacobian (4.27) has all its eigenvalues with negative real part. We can conclude that for such values of ε, the point $\tilde{Q}_I = \mathbf{0}$ is a locally exponentially stable fixed point for (4.22). It follows that the fixed point of (4.16) is $\tilde{Q}_I = \mathbf{0}$, along with

$$g^{\mathrm{eq}} = G(\varepsilon, \tilde{Q}_I = \mathbf{0}) .$$

Since $g = G(\varepsilon, \tilde{Q}_I)$ is a continuous function of $\tilde{Q}_I$, the local exponential stability of $\tilde{Q}_I = \mathbf{0}$ implies the local exponential stability of g^{eq}. This in turn is equivalent to the local exponential stability of the fixed point (4.12) expressed in terms of the original varibles E_L and E_I.

Part 4 (Bound (4.13) **on the error term):** If we define the quantity k^{eq} such that

$$g^{eq} = \begin{bmatrix} X_{LL} \\ X_{LI} \end{bmatrix} \mathrm{diag}^{-1}(\mathbb{1} + M_L\tilde{\eta})Q_L, + \frac{1}{\tilde{E}_N^2}k^{\mathrm{eq}}$$

Then the fixed point can be expressed in terms of the original variables as

$$\begin{bmatrix} E_L^{eq} \\ E_I^{eq} \end{bmatrix} = \tilde{E}_N(\mathbb{1} + M\tilde{\eta}) + \frac{1}{\tilde{E}_N} \begin{bmatrix} X_{LL} \\ X_{LI} \end{bmatrix} \operatorname{diag}^{-1}(\mathbb{1} + M_L\tilde{\eta})Q_L + \frac{1}{\tilde{E}_N^3} k^{\text{eq}} \,,$$

And applying the same proof carried out in Theorem 3.1 we can show the bound (4.13). This completes the proof of Theorem 4.1. □

4.3 Numerical case study of the fixed point

In this section we test the results obtained in Theorem 4.1 on an islanded version of the standard IEEE 37 distribution network. The description of this grid has already been given in the numerical case study for the approximate solution of the reactive power flow equations. We remind that the nominal operating voltage for this grid is 4.8kV. The sources in this network are DC/AC inverters, whose voltage magnitudes are governed by the quadratic droop controller (4.2). We simulate the resulting differential-algebraic system (4.9) for different values of $\tilde{E}_N$ and study:

a) the threshold $\tilde{E}_N^{\min}$ above which the fixed point (4.12) exists and is stable;
b) the accuracy of the approximated fixed point expression (4.12). We consider two variations on the approximation presented in (4.12): in the *approximation* 1 we set $k^{\text{eq}} = \mathbf{0}$ in (4.12); the approximation *approximation* 2 is instead

$$\begin{bmatrix} E_L^{eq} \\ E_I^{eq} \end{bmatrix} = \tilde{E}_N(\mathbb{1} + M\tilde{\eta}) \,.$$

To quantify the error between the true fixed point E_{nonlin}^{eq} of the nonlinear system and the approximations 1 and 2, we introduce the

relative approximation errors

$$r_i := \frac{\|E^{eq}_{\text{nonlin}} - E^{eq}_{\text{approx},i}\|_\infty}{E_N}\,, \quad i \in \{1,2\}\,,$$

where the vector E includes both the loads and the inverters voltages.

Given this setup, we expect the numerical results to be qualitatively similar to the ones found in Section 3.4.

The threshold $\tilde{E}_N^{\min}$ above which a stable high-voltage fixed point exists was found by simulation to be roughly 850V, well below the muli-kV range in which the system is operated, but above the one found in Section 3.4. This holds for initial conditions equal to the reference baseline voltages. If instead we decrease the initial voltages to be ten times smaller that the reference baseline voltages, we find that the threshold becomes 9kV. The explanation of this is given by the fact that Theorem 4.1 proves the *local* stability of the fixed point. Looking back at the proof, it can be deduced that the attraction region for g increases when $\tilde{E}_N$ increases. Therefore initial conditions far from the fixed point require the reference baseline voltages to be bigger in order for the fixed point to attract their trajectories. From now on we refer to initial conditions equal to the reference baseline voltages; this is the relevant case for the normal operating point of a network.

Figure 4.2 reports the relative approximation errors r_1 and r_2 for the approximations 1 and 2 in the IEEE 37 network, for different values of $\tilde{E}_N$.

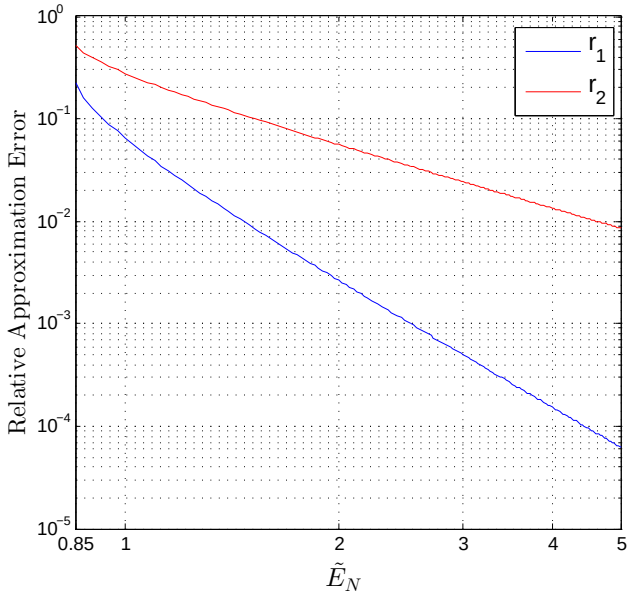

Figure 4.2: The log-log plot of the relative errors of approximation 1 and 2, computed numerically for different values of the baseline source voltage E_N. The threshold $\tilde{E}_N^{min} = 850\text{V}$ is marked.

Note first that both relative approximation errors decrease rapidly as $\tilde{E}_N$ grows. In particular at the 4.8kV nominal operating voltage of the network, the relative error using both approximations is below 0.1%, with the accuracy of approximation 1 being below 0.01%.
In Figure 4.3 for each E_N we report the approximation error 1 multiplied by E_N^3 and the approximation error 2 multiplied by E_N. The fact that the two curves tend to a constant value shows that the approximation error 1 tends to zero exactly as $1/E_N^3$ and the approximation error 2 tends to zero exactly as $1/E_N$. This corresponds to the results found in Section 3.4 and hold also here because of the definitions of the two approximations used.

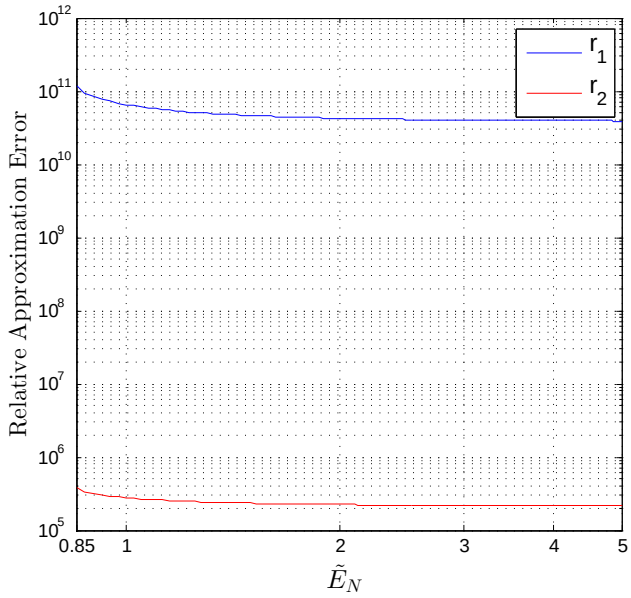

Figure 4.3: The log-log plot of the errors scaled by appropriate powers of E_N shows the asymptotic behavior of the errors.

Chapter 5

Conclusions

In this work we have presented novel analytic expressions for the approximate solution of the decoupled reactive power flow equations. Aside from the clear application in transmission networks, we have demonstrated the flexibility of our result by using it to study the behavior of droop-controlled inverters in an islanded microgrid. Through simulation, we have demonstrated that our results are practical and extremely accurate in real power networks. Future work in this direction seeks to examine more closely the role of the voltage spread η in the difference between the two approximations analyzed in Section 3.3; we also want to try to further relax the assumption of small angular differences. It is of theoretical interest to analyze the attraction region for the fixed point, both in a numerical and analytical way, starting from the proof of Theorem 4.1.

We further envision an extensive set of case studies, with the goal of demonstrating conclusively the usefulness of this approximation in power system planning and operation.

Appendix A

Matlab code

We report in the following the Matlab code we have used for our simulations:

```
function errors_comparison

% clear all
% close all

grid = 1; % 0 for parallel, 1 for IEEE_37

if (grid==0)
    E_N_vec = 8:0.5:70; % parallel case
else
    E_N_vec = 1000:25:5000; % IEEE_37 suggested by
        John (4700-5000)
end

diff_sim_approx =          zeros(1,length(E_N_vec));
diff_sim_exact =           zeros(1,length(E_N_vec));
diff_approx_exact =        zeros(1,length(E_N_vec));
diff_bad_approx_exact =    zeros(1,length(E_N_vec));
diff_sim_bad_approx =      zeros(1,length(E_N_vec));
```

```
19 bound_vec =                zeros(1,length(E_N_vec));
20
21 % loop to obtain the errors vectors for different
       E_N
22 for count=1:length(E_N_vec)
23
24     E_N = E_N_vec(count);
25     E_N
26
27     to_be_compared = dae_solver(E_N);
28
29     diff_sim_approx(count) = max(abs(to_be_compared
           (:,1)-to_be_compared(:,2)))/E_N;
30     diff_sim_bad_approx(count) = max(abs(
           to_be_compared(:,1)-to_be_compared(:,3)))/E_N
           ;
31     bound_vec(count) = to_be_compared(end,end)/E_N;
32
33     if (grid==0)
34         diff_bad_approx_exact(count) = max(abs(
               to_be_compared(:,3)-to_be_compared(:,4)))
               /E_N;
35         diff_sim_exact(count) = max(abs(
               to_be_compared(:,1)-to_be_compared(:,4)))
               /E_N;
36         diff_approx_exact(count) = max(abs(
               to_be_compared(:,2)-to_be_compared(:,4)))
               /E_N;
37     end
38 end
39
40 % we plot the errors obtained
```

```
41 figure
42
43 if (grid==0)
44     loglog(E_N_vec,diff_approx_exact,'b');
45     hold on
46     loglog(E_N_vec,diff_bad_approx_exact,'r');
47 else
48     loglog(E_N_vec,diff_sim_approx,'b');
49     hold on
50     loglog(E_N_vec,diff_sim_bad_approx,'r');
51 end
52
53 % we show the bound
54 % hold on
55 % plot (E_N_vec,bound_vec,'g');
56
57
58 if (grid==0)
59     xlim([3 50])
60 end
61 % ylim([10^(-4) 10^(-5)])
62
63 xlabel('$\tilde{E}_N$','Interpreter','LaTex','
       FontSize',14)
64 ylabel('Relative Approximation Error','FontSize',13,
       'Interpreter','latex')
65 h=legend('\delta_1','\delta_2','Interpreter','latex'
       );
66 set(h,'FontSize',13);
67
68
69
```

```
70      function to_be_compared = dae_solver(E_N)
71      % solves the differential (algebraic)
            numerically
72
73      if (grid==0) % for the parallel case
74
75
76          n_I = 1;
77          n_L = 1;
78          L = [1 -1; -1 1]; % one inverter
79          % L = [2 -1 -1; -1 1 0; 0 -1 1]; % two
                inverters
80          Q_L = -2;
81
82          tau_I = eye(n_I);
83          tau_L = 0.01 * eye(n_L);
84
85      else % for the IEEE 37 case
86
87          data = load('IEEE_37.mat');
88          B = data.B(data.perm,:);
89          n_I = length(data.InverterLabels);
90          n_L = length(data.Labels) - n_I;
91          L = -imag(B * diag(data.Weights) * B');
92
93          Q_L = - 20000 - 60000 * rand(n_L,1); %
                IEEE_37
94          Q_L =     1.0e+04 * [   -5.1649; -7.9818;
                -7.4559;    -5.9109;    -2.7887;    -6.3463;
                    -5.7999;    -6.7851;    -6.4891;
                -2.2053;            -5.0167;    -4.2553;
                -7.3594;    -3.0971;    -2.6949;    -4.4141;
```

```
                -6.0875;    -6.5023;    -6.3063;
            -6.3975];
95
96          tau_I = eye(n_I);
97          tau_L = 0.01 * eye(n_L);
98
99      end
100
101     % quadratic droop gains
102     C_I = 0.5 * eye(n_I);
103
104     % definition of E_J (starting from E_N)
105
106     % eta = 0.1*rand(n_I,1);
107     if (grid == 0)
108         eta = 0.05;
109     else
110         eta = [0.0352; 0.0154; 0.0406; 0.0102;
                0.0744; 0.0465; 0.0162; 0.0026; 0.0417;
                0.0854; 0.0606; 0.0171; 0.0739; 0.0301;
                0.0757; 0.0348];
111     end
112     E_J = E_N * (1 + eta); % we add at most the 10
            percent for each E_J
113
114
115     % exact expression of the equilibrium (only for
            the parallel case)
116     if(grid==0)
117         L_LL = L(1:n_L,1:n_L);
118         L_LI = L(1:n_L,n_L+1:end);
119         L_IL = L_LI';
```

```
120         L_II = L(n_L+1:end,n_L+1:end);
121
122         L_red = L_LL - L_LI * inv(C_I+L_II) * L_IL;
123         W_1 = - inv(L_red) * L_LI * inv(C_I + L_II)
                * C_I;
124         E_avg = W_1 * E_J;
125
126         Q_crit = 1/4 * L_red * E_avg^2;
127         E_0_sol = E_avg / 2 * (1 + sqrt(1 + Q_L /
                Q_crit));
128         E_I_sol = (C_I .* E_J - L_LI * E_0_sol) ./ (
                C_I - L_LI);
129     end
130
131
132     tspan = [0,10];
133     E_0 = E_N * ones(n_I + n_L,1); % we start from
            good initial conditions;
134     mass_matrix = blkdiag(tau_L,tau_I);
135     odeset('Mass',mass_matrix);
136     odeset('RelTol',10^(-6));
137     odeset('AbsTol',10^(-6));
138
139     [~,E_plot] = ode15s(@diff,tspan,E_0);
140
141     % matrices needed to find the approximate
            equilibrium
142     X = inv(L + blkdiag(zeros(n_L,n_L),C_I));
143     X_LL = X(1:n_L,1:n_L);
144     X_LI = X(1:n_L,n_L+1:end);
145     X_IL = X_LI';
146     X_II = X(n_L+1:end,n_L+1:end);
```

```
147
148     M_L = X_LI * C_I;
149     M_I = X_II * C_I;
150     M = [M_L; M_I];
151
152     g_lim = - [X_LL; X_IL] * inv(diag(1 + X_LI * C_I
            * eta)) * diag(X_LI * C_I * eta) * Q_L;
153
154     E_approx =      E_N + E_N * M * eta + 1/E_N * [
            X_LL; X_IL] * Q_L + 1/E_N * g_lim;
155     E_bad_approx = E_N + E_N * M * eta + 1/E_N * [
            X_LL; X_IL] * Q_L;
156
157     % we compute the bounds on the error term
158
159     alpha = 4*sqrt(2)*max(sqrt(sum(abs(M).^2,2)))*
            max(sqrt(sum(abs(X).^2,2)));
160     beta = 4*sqrt(2)*max(sqrt(sum(abs(X).^2,2)))^2;
161     bound = alpha*norm(eta)*norm(Q_L)+beta*norm(Q_L)
            ^2/(E_N^2);
162     bound = bound*ones(n_L+n_I,1);
163
164     if (grid==0)
165         E_exact = [E_0_sol; E_I_sol]; % in the
                parallel case we insert the exact
                expression
166         to_be_compared = [E_plot(end,:)' E_approx
                E_bad_approx E_exact bound];
167     else
168         to_be_compared = [E_plot(end,:)' E_approx
                E_bad_approx bound];
169     end
```

```
170
171         function dE = diff(~,E)
172         % computes the left-hand side of the
                differential system
173
174             E_I = E(n_L+1:end);
175             dE = [Q_L; C_I * diag(E_I)*(E_J - E_I)]
                    - diag(E)*L*E;
176
177         end % of diff
178
179     end % of dae_solver
180
181 end % of errors_comparison
```

Bibliography

[1] S. Bolognani and S. Zampieri, "A distributed control strategy for reactive power compensation in smart microgrids," vol. 58, no. 11, 2013, to Appear.

[2] A. Araposthatis, S. Sastry, and P. Varaiya, "Analysis of power-flow equation," *International Journal of Electrical Power & Energy Systems*, vol. 3, no. 3, pp. 115–126, 1981.

[3] I. Dobson, "Observations on the geometry of saddle node bifurcation and voltage collapse in electrical power systems," vol. 39, no. 3, pp. 240–243, 1992.

[4] H. Chiang and M. Baran, "On the existence and uniqueness of load flow solution for radial distribution power networks," vol. 37, no. 3, pp. 410–416, 1990.

[5] F. Wu and S. Kumagai, "Steady-state security regions of power systems," vol. 29, no. 11, pp. 703–711, 1982.

[6] J. Thorp, D. Schulz, and M. Ilić-Spong, "Reactive power-voltage problem: conditions for the existence of solution and localized dis-

turbance propagation," *International Journal of Electrical Power & Energy Systems*, vol. 8, no. 2, pp. 66–74, 1986.

[7] M. Ilić, "Network theoretic conditions for existence and uniqueness of steady state solutions to electric power circuits," in *IEEE International Symposium on Circuits and Systems*, San Diego, CA, USA, May 1992, pp. 2821–2828.

[8] B. C. Lesieutre, P. W. Sauer, and M. A. Pai, "Existence of solutions for the network/load equations in power systems," vol. 46, no. 8, pp. 1003–1011, 1999.

[9] P. Kundur, *Power System Stability and Control*, 1994.

[10] F. Dörfler and F. Bullo, "Novel insights into lossless AC and DC power flow," Vancouver, BC, Canada, Jul. 2013, to appear.

[11] J. Machowski, J. W. Bialek, and J. R. Bumby, *Power System Dynamics*, 2nd ed., 2008.

[12] J. A. P. Lopes, C. L. Moreira, and A. G. Madureira, "Defining control strategies for microgrids islanded operation," *IEEE Transactions on Power Systems*, vol. 21, no. 2, pp. 916–924, 2006.

[13] M. C. Chandorkar, D. M. Divan, and R. Adapa, "Control of parallel connected inverters in standalone AC supply systems," *IEEE Transactions on Industry Applications*, vol. 29, no. 1, pp. 136–143, 1993.

[14] J. W. Simpson-Porco, F. Dörfler, and F. Bullo, "Voltage stabilization in microgrids using quadratic droop control," Florence, Italy, Dec. 2013, to appear.

[15] M. E. J. Newman, *Networks: An Introduction*, 2010.

[16] R. A. Horn and C. R. Johnson, *Topics in Matrix Analysis*, 1994.

[17] R. Abraham, J. E. Marsden, and T. S. Ratiu, *Manifolds, Tensor Analysis, and Applications*, 2nd ed., ser. Applied Mathematical Sciences, 1988, vol. 75.

[18] M. Guarnieri, *Elementi di elettrotecnica circuitale.* Edizioni Progetto, Padova, 2008.

[19] S. Lissandron, "Tecniche di controllo droop per la gestione di microreti isolate a bassa tensione," in *Master's Thesis*, Università degli Studi di Padova, 2012.

[20] D. Carlson and H. Schneider, "Inertia theorems for matrices: The semidefinite case," *Journal of Mathematical Analysis and Applications*, vol. 6, pp. 430–446, 1963.

[21] H. Goldstein, C. Poole, and J. Safko, *Classical Mechanics*, 3rd ed., 2000.